ACS APPLIED MATERIALS & INTERFACES

Research Article

www.acsami.org

Enhancing Adhesion of Elastomeric Composites through Facile Patterning of Surface Discontinuities

Samuel A. Pendergraph,[†] Michael D. Bartlett, Kenneth R. Carter,* and Alfred J. Crosby*

Department of Polymer Science and Engineering, University of Massachusetts, 120 Governors Drive, Amherst, Massachusetts 01003-9265, United States

Supporting Information

ABSTRACT: Patterning interfaces can provide enhanced adhesion over a projected area. However, careful consideration of the material properties and geometry must be applied to provide successful reversible adhesives. We present a simple method to use patterned, elastomeric fabric composites to enhance the shear adhesion strength by nearly 40% compared to a non-patterned sample. We describe how this enhancement depends on the pattern geometry, the velocity dependence of the adhesive materials, and the controlled displacement rate applied to the interface. Through these observations, we discuss strategies for improving reversible adhesives.

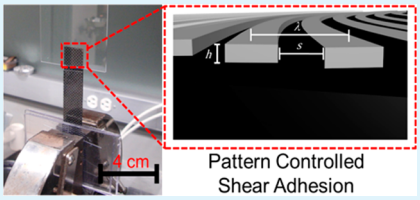

KEYWORDS: *adhesion, patterning, lithography, composites*

INTRODUCTION

The design of robust, reversible adhesives has been studied with immense interest in recent years through modification of interfacial chemistry and geometry. One example is bioinspired adhesives that mimic the fibrillar features found on the adhesive toe pads of organisms such as the Tokay Gecko to control adhesion.[1−6] Aside from long, thin compliant structures, other topographies, such as wrinkles and interlocking structures, have also been implemented to control adhesion strength.[7−15] Studies have been conducted with normal, peel, and shear adhesion of bioinspired surfaces[1−3,5,16−18] as well as patterned soft materials in general.[19−21] Although advantages have been highlighted for all of these soft fibrillar-like structures, limitations are also acknowledged in terms of their overall loading capacity. Specifically, patterned structures that are composed of soft materials can make intimate contact but lack high stiffness to achieve high loads.

Recently, elastomeric fabric composites have been demonstrated to achieve high shear adhesion forces while remaining reversible.[22,23] This advantageous balance of properties arises because the soft elastomer can establish intimate contact on the micrometer and submicrometer length scales while also allowing for the fabric to drape and maintain contact at larger sizes on non-ideal substrates.[24] In addition, the rigid fibers of the fabric minimize deformation, leading to a high adhesive force capacity. Adhesion through these fabric composites relies primarily on material elasticity and reversible non-specific surface interactions such as van der Waals forces, thus reducing material constraints on the design of the adhesive. However, this general design concept has the potential for further modification of surface topography to add increased functionality.

In recent work by Chaudhury and co-workers, they described how incisions and discontinuities in a film can lead to an increase in peel adhesion.[16] They examined the role of line discontinuities on the effect of crack propagation in peel adhesion of elastomers and demonstrated that crack blunting can lead to substantial adhesion improvements. Specifically, they highlight two factors: first, the orientation of the line incisions should be orthogonal to the peel direction (or parallel to the crack front). Second, the incision spacing should be less than a critical stress decay length. By understanding how the crack propagation occurred in these types of patterns, the researchers devised more complex topographies to enhance the adhesion through a crack blunting mechanism.[16]

Here, we expand the general design concept of elastomeric fabric adhesives through surface patterning to demonstrate further control of shear adhesion force capacity. Specifically, we demonstrate the facile use of topographical line patterns to enhance shear adhesion strength up to almost 40% compared to the non-patterned composite material. By orienting the line patterns orthogonal to the direction of crack propagation, higher adhesion was achieved by slowing catastrophic failure of the interface through crack blunting. To our knowledge, this is the first report of implementing patterned elastomeric fabric composites to demonstrate robust, enhanced adhesive behavior.

EXPERIMENTAL SECTION

Materials. Poly(dimethylsiloxane) (PDMS) elastomer Sylgard 184 (referred in this paper as x-PDMS) was purchased from Dow Corning. Plain-weave carbon fiber 1-k fabric was purchased from Composite Envisions. Rewritable compact discs (CD) and digital video discs (DVD) were purchased from Verbatim.

Instrumentation. Mechanical testing was performed on an Instron 4400R and 5500R with a 50 N load cell. Atomic force microscopy (AFM) was performed on a Digital Instruments Nanoscope III in tapping mode under ambient conditions. Contact adhesion testing and

Received: January 29, 2014
Accepted: April 14, 2014
Published: April 14, 2014

   dx.doi.org/10.1021/am5006546 | ACS Appl. Mater. Interfaces 2014, 6, 6845−6850

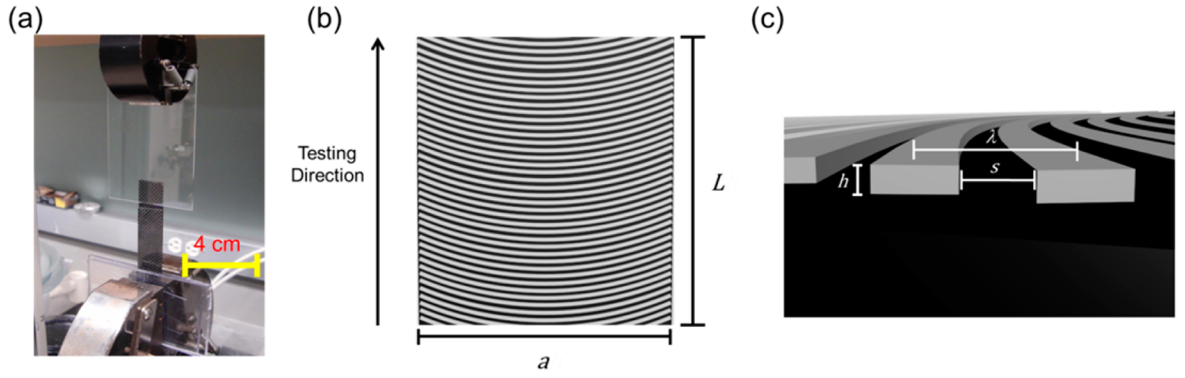

Figure 1. (a) Photograph of the testing apparatus with sample. The patterned area of the sample was attached to the glass. (b, c) Schematic of the top view of the patterned substrate (not to scale) (b) and side perspective view of the line features (c).

adhesion testing with microscope imaging was performed on a custom contact adhesion testing instrument.[25]

Fabrication of Patterned Fabric Composites. CD and DVD patterned fabric composites were fabricated by literature procedures.[24] Briefly, the CD mold was fabricated by removing the foil on top of the CD and then washing immediately with copious amounts of isopropanol. After the organic ink was removed, the sample was dried with a stream of air. For DVD molds, the disc was separated into two pieces, and the patterned section was washed with copious amounts of isopropanol. The dimensions of the molds are shown in Figure S1. Both CD and DVD discs have a radius of 6 cm. Sylgard 184 was mixed at a 5:1 prepolymer/crosslinker ratio and degassed to remove air bubbles. The ratio of 5:1 was used because the ratio between the critical energy release rate (G_c) and the elastic modulus (E) was greater than the height of the CD/DVD features but less than the spacing of adjacent lines. Afterward, a mold was then placed on a sheet of poly(ethylene terephthalate) (PET). Sylgard 184 was then poured into the mold. Next, a piece of plain-weave carbon fiber was placed on top of the Sylgard 184. More Sylgard 184 was poured on top of the fabric until it was completely covered, and another piece of PET was placed on top of the resin-covered fabric. The composite was allowed to cure for 72 h at room temperature followed by a 1 h cure at 70 °C. Finally, the mold was removed, leaving a patterned fabric composite. For the case of the non-patterned substrate, Sylgard 184 was poured on top of the carbon fiber fabric and placed between two sheets of PET and cured in the same method as that for the patterned composites. A general schematic of the fabrication of the patterned substrates is shown in Figure S2.

Lap Shear Adhesion Testing of Fabric Composites. Fabric composites were tested for adhesion testing by clamping the end opposite of the testing area between two pieces of polycarbonate. The patterned area size was kept to approximately 2 cm^2 for all samples. A distance of 4 cm between the bottom of the patterned feature and the top of the clamping area was held constant through all adhesion testing. The polycarbonate grips were then clamped into to the fixed end of the Instron. Next, a piece of glass was cleaned by manual washing with commercial soap and then dried under a stream of air. The cleaned piece of glass was then clamped into the moving head of the Instron setup. The testing area was then attached by hand to the glass slide, and the testing was then initiated with varying testing velocities.

Adhesion Testing of Fabric Composites with Microscope Imaging. To image the propagation of interfacial failure at sufficiently high resolution, lap shear adhesion tests were performed on a custom-designed instrument that was fixed below an optical microscope. Specifically, fabric composites were tested by clamping a cleaned 75 × 55 mm glass slide to a rigid stand fixed to a breadboard table. The unsupported edge of glass slide was then placed underneath the microscope objective (2.5× magnification) with a Zeiss AxioTech Vario optical microscope. The bottom of the fabric composite was clamped to another rigid stand, which was also fixed to a breadboard table, and the testing region of the composite was brought into contact on the bottom side of the glass slide. After the sample was in focus, the sample was pulled horizontally at a testing velocity of 5 mm/min.

Modulus Measurement of x-PDMS. Mechanical properties of x-PDMS were evaluated through tensile testing on an Instron 4400. The samples were cut into dog-bone samples with a gauge length of 26 mm in length and 4.6 mm in width and were pulled at 5 mm/min.

Determination of G_c for Bulk x-PDMS. To provide a baseline measurement of the adhesion between the x-PDMS elastomer and glass, measurements of the mode I critical energy release rate, G_c, were performed using a custom-built contact adhesion testing instrument. A glass hemispherical probe (radius = 5 mm) was brought into contact with the x-PDMS substrate at rate of 5 mm/min to a load of 10 mN and then withdrawn at the same rate while the contact force, relative displacement, and contact area were monitored continuously. An effective G_c was then determined from the critical pull-off force using the JKR relationship

$$G_c = \frac{2P}{3\pi R} \quad (1)$$

where R is the radius of curvature of the glass probe and P is the maximum tensile load at adhesive separation. Although it is known that G_c is velocity-dependent for elastomer interfaces in general, for this study, we limit our characterization to a single velocity, which is appropriate for drawing comparisons to the lap shear experiments.

RESULTS AND DISCUSSION

Shear adhesion experiments were performed on five different samples: a non-patterned plain-weave carbon fiber/x-PDMS sample and two rectangular patterns with different spacing, each in two different orientations. For the patterned samples, we defined the lines as being oriented "parallel" when the lines were oriented along the testing directions and "orthogonal" when the lines were perpendicular to the testing direction. The fabric composites patterned from the DVD features had a periodicity (λ) of approximately 750 nm, a depth (d) of 150 nm, and a spacing width (s) of approximately 350 nm (Figure 1c). The CD features had a periodicity of approximately 1500 nm, a depth of 200 nm, and a spacing width of approximately 600 nm (AFM images of molds are shown in Supporting Information, Figure S1). The use of the CD and DVD patterns enabled the rapid and reliable replication of these submicrometer dimensions.

Because the patterns originated from a circular pattern, we needed to consider how the orientation of the lines changes as a function of the sample size and geometry. The sector angle gives the range of angles that the line will deviate from the testing direction. The sector angle can be expressed as a function of the diameter of the CD or DVD template (D) and the chord length (a)

$$\theta = 2\sin^{-1}\left(\frac{a}{D}\right) \quad (2)$$

The chord length for the orthogonal example is related to the width, and conversely, the length of the sample, the parallel orientation. The angle of an arbitrary line relative to a given position of the sample was determined because both a and D were known in the sample construction (Figure 2). The angle

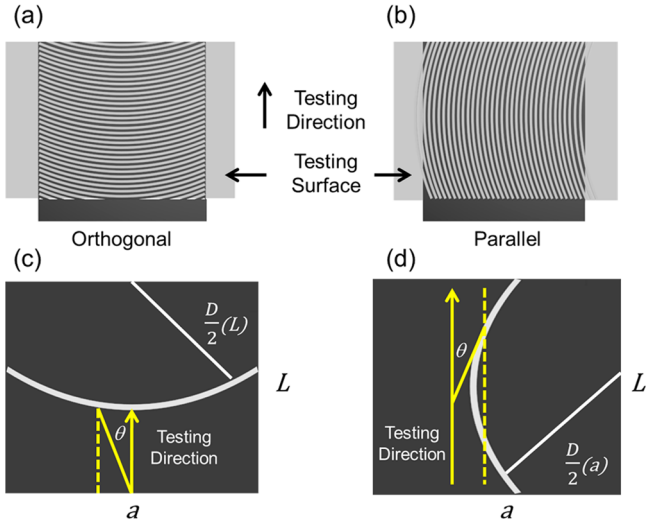

Figure 2. Angle of the applied force to the line relative to position on the substrate. The angle of a given location of the line can be related to the sector angle of the CD or DVD template through eq 2.

of the line relative to an idealized line direction typically varied from 0 to ±17.5° (corresponding to a total sector angle of 35°), depending on the radius of curvature of the line and relative position in the chord length. A total sector angle of 90° or higher (from an idealized line direction) would lead to line features on a single pad that have both parallel and orthogonal orientations. This non-negligible mixture of line orientations would occur at a/D values between 0.806 and 1; for our samples, the values for a/D were limited between 0.075 and 0.10. Therefore, despite the curvature of the lines, at the size scales investigated here, the two line arrangements remained distinct from each other in terms of the angles exhibited during testing.

After the patterns were fabricated, the samples were clamped and the testing area was applied to a glass slide until the disappearance of the diffraction grating (Figure 1a). The disappearance of the light diffraction indicated intimate contact, where both the top and bottom of the line features were in contact and remained stable until the sample was strained. The sample was then loaded until a maximum critical force (F_c) was reached and the adhesive subsequently separated from the substrate completely. Representative plots of the five different patterned surfaces are shown for the 5 mm/min testing rate along with the corresponding adhesive stress capacities (F_c/A, where A is the projected contact area) in Figure 3c,d.

The orthogonal patterns demonstrated different shear adhesion values compared to the parallel and the non-patterned samples. The CD and DVD samples exhibited a 20 and 37% increase in adhesion, respectively, relative to the non-patterned substrate. To discern the source of the enhancement of the orthogonally patterned features, we first implemented a

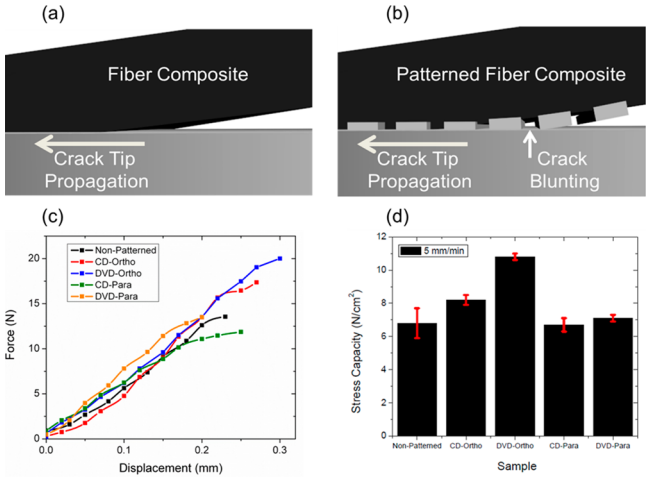

Figure 3. (a) Schematic of crack propagation of an unpatterned fabric composite. (b) Crack blunting for an orthogonal patterned fabric composite. (c) Representative force vs displacement plots at 5 mm/min for the five different types of fabric composite substrates. (d) Resulting adhesive stress capacity for the five different orientations for a test velocity of 5 mm/min. The error bars correspond to the scatter for five tests in each pattern orientation.

previously reported general force scaling relationship for reversible adhesion[22,23]

$$F_c \sim \sqrt{G_c}\sqrt{\frac{A}{C}} \quad (3)$$

where F_c is the critical adhesive force, G_c is the critical strain energy release rate, A is the area of contact, and C is the compliance of the sample in the loading direction. From our previous work with elastomeric fabric composites, we have shown that adhesive failure, or interfacial fracture, occurs in a single step (i.e., unstable crack propagation) when F_c is reached.[22] Because the samples had identical resin materials and processing conditions, G_c is unlikely to be the differentiating component to the adhesion discrepancies. The contact area (A) and compliance of the samples (C) was similar and relatively invariant, even with varying velocities (Figure S3), and therefore is unlikely to be the source of variance in the adhesion performance. We attribute the change in force capacity to the ability of the orthogonally patterned samples to initially blunt crack growth (Figure 3a). This blunting, or slowing of crack propagation, increases the loading time, which allowed the force to continue to climb for fixed displacement rate loading conditions before catastrophic interfacial failure proceeds.

One requirement of this mechanism of adhesion enhancement of patterned surfaces is that the interfacial cracks should act discretely in order to impede propagation and for force reinitiation to occur. Patterns act discretely if they are spaced at distances greater than the distance over which adhesives interactions occur, δ_c, which is defined by[24]

$$\delta_c \approx \frac{G_c}{E} \quad (4)$$

where E is measured through tensile measurements for a given velocity of loading. From the hemispherical contact adhesion measurements conducted at 5 mm/min, G_c was found to be 0.44 ± 0.07 J/m^2 for the elastomer pads. The elastic modulus of the bulk x-PDMS elastomer was measured to be ~1.7 MPa

dx.doi.org/10.1021/am5006546 | ACS Appl. Mater. Interfaces 2014, 6, 6845−6850

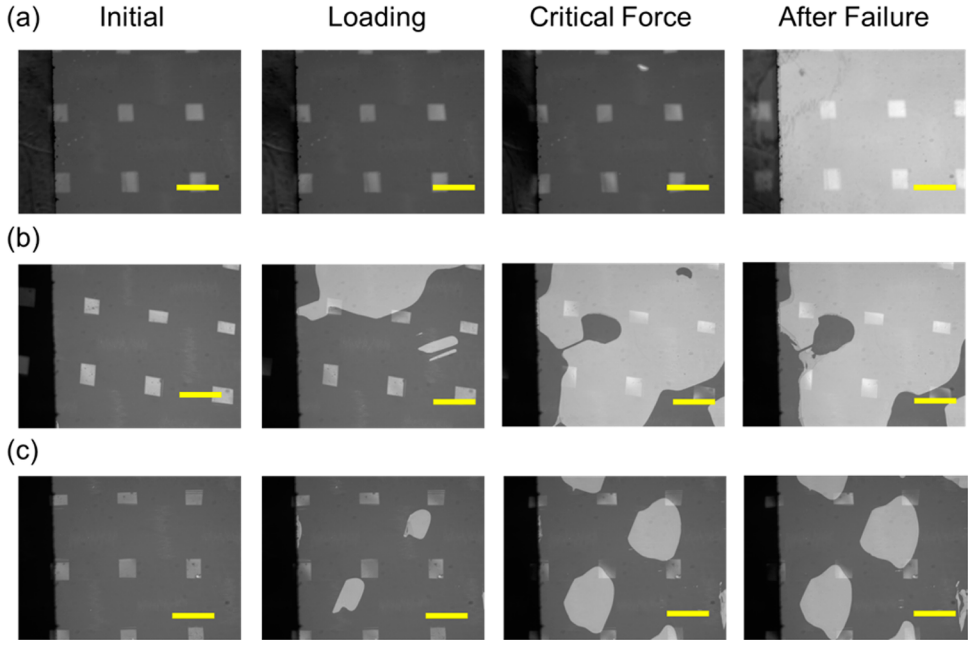

Figure 4. Optical micrograph images of shear testing for the non-patterned fabric composite (a), CD parallel configuration (b), and CD orthogonal configuration (c). The first column is the initial state of all three samples, the second column is an image of the sample while loading, the third column is the sample at the critical force for each configuration, and the fourth column is the sample after failure has occurred at the interface. The open squares are gaps in the fabric between adjacent fiber bundles. The scale bars are 1 mm.

from uniaxial tensile measurements. Substituting these values in to eq 4, we found that the critical length scale was approximately 260 nm. This length was less than the spacing (s) of the patterned features, suggesting that the lines acted discretely. Furthermore, because δ_c was greater than the depth of the patterned features (h), once troughs create contact with the glass they should not spontaneously separate, which is consistent with our observations. At these testing velocities, these patterns acted discretely but made equivalent contact area to a non-patterned substrate. The material properties of x-PDMS and geometric dimensions of the patterns gave some insight into the enhanced adhesion mechanism.

The results for 5 mm/min testing rate prompted the examination of the interface during testing. In Figure 4, we show crack propagation images for the non-patterned sample and the two CD line configurations. In the non-patterned sample, the entire area was maintained until the critical force was reached, and then the entire interface failed instantaneously. The crack propagation occurred in the direction parallel to the testing direction. In the parallel configuration, there was partial separation of the interface, where the separation grew anisotropically along the direction of the lines. The interface then failed followed by sliding of the elastomeric interface. Lines oriented parallel to the crack propagation direction did not alter, or slow, the unstable adhesive failure. Furthermore, similar to the results of Chung and Chaudhury, we observed no increased interfacial critical pull-off stress for the lines oriented parallel to the crack propagation direction.[16] In the orthogonal configuration, we again saw anisotropic, partial separation of the interface as the sample was being loaded. After the critical force was reached, the sample began to slide similar to the parallel example. Although some separation occurs in the direction of propagation, the lines generally diverted the crack growth. This crack blunting mechanism allowed the adhesive to remain in contact for a longer duration during loading at fixed displacement rates and thus the orientation gave rise to larger adhesive stress capacities.

To explore the crack blunting mechanism further, the testing velocity dependence for these systems was investigated. In Figure 5, four different testing velocities were implemented, and the corresponding adhesive stress capacities are shown. In the intermediate velocity region (5 and 25 mm/min), we observed adhesion enhancement for the orthogonal configuration in both the DVD and CD line patterns. At these velocities, the elastomeric interface appeared to be affected by the pattern orientation. The contact area was maintained for longer loading

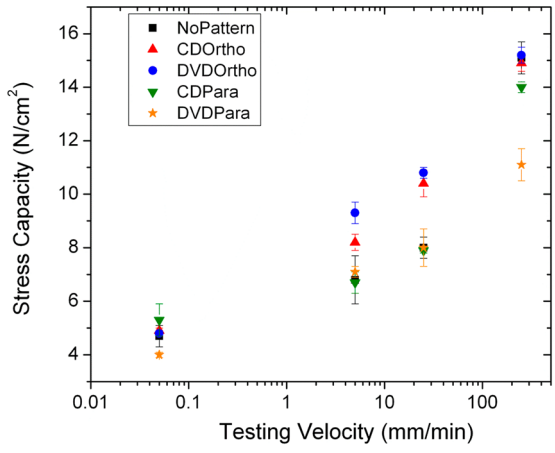

Figure 5. Adhesive stress capacity of the samples vs testing velocity over four different testing velocities (0.05, 5, 25, and 250 mm/min). Each point represents the average adhesive stress capacity over five tests, with the error bars representing the scatter. Adhesion enhancement for the two orthogonal configurations can be seen in 5 and 25 mm/min; however, nearly all adhesive pads produce equivalent adhesive stress capacities, within error, at the two extreme testing velocities of 0.05 and 250 mm/min.

time intervals and thus the load in the sample can be increased for the patterned substrates. For the lowest velocity, we believe that the enhancement was not observed because the crack velocity was moving at a much greater rate than the loading of the sample. Therefore, the interface failed before the load can increase; thus, higher pull-off forces were not observed. In the highest testing velocity, the adhesion enhancement disappeared because the crack propagation was driven by the testing velocity. The instrument velocity was likely faster than the crack propagation velocity. Given a constant contact area, all samples were given equal time to load and thus have approximately the same adhesive stress capacity. Furthermore, because G_c has been shown to increase as a function of velocity,[26] it is possible that the increase in G_c would cause the line discontinuities no longer to be discrete. Coupling of the features would render them ineffective in crack blunting. It is important to note that despite the lack of differentiating behavior in the patterned substrates, a maximum F_c was achieved at 250 mm/min.

From our previous work on the adhesion of elastomeric fabric composites, the improvements with these composites should be scalable to larger adhesive pad sizes as long as the a/D ratio is sufficiently small. Alternatively, several adhesives of smaller areas can be coupled to create a single pad with a larger area.[21] The advantage of this strategy is that it potentially attenuates the demand for creating a large area pattern, which would increase the probability of defects. The combination of the elastomeric fabric composites allows low cost and facile patterning on the testing surface as well as flexibility in terms of the geometry that can be used to create robust, reversible adhesives.

CONCLUSIONS

We have evaluated the shear adhesion of patterned elastomeric fabric composites. We implemented a simple fabrication procedure that utilized line features similar to patterns found in nature. The orientation of the patterning proved to be critical, where a line arrangement orthogonal to the testing direction is essential for adhesion enhancement. At intermediate velocities, adhesion enhancement of up to 37% was observed with orthogonally patterned lines compared to adhesive values from equivalent non-patterned fabric composites. Furthermore, we demonstrated how adhesion enhancement was a function of the fixed displacement rate, the pattern geometry and orientation, and the elastomer materials properties. In particular, the crack blunting mechanism allowed the composite adhesive to remain in contact longer when the displacement rate was greater than but near the slowed debonding crack velocity of the adhesive pad, resulting in adhesion enhancement by allowing the force to climb at intermediate testing velocities. These results will guide the design of patterned adhesives to create robust and reversible adhesives.

ASSOCIATED CONTENT

Supporting Information

AFM images of the molds used for imprinting, a general fabrication schematic, and the plot of system stiffness versus testing velocity. This material is available free of charge via the Internet at http://pubs.acs.org.

AUTHOR INFORMATION

Corresponding Authors

*(K.R.C.) E-mail: krcarter@polysci.umass.edu.

*(A.J.C.) E-mail: crosby@mail.pse.umass.edu.

Present Address

†(S.A.P.) KTH Royal Institute of Technology, Department of Fibre and Polymer Technology, Division of Coatings Technology, SE-100 44 Stockholm, Sweden.

Notes

The authors declare no competing financial interest.

ACKNOWLEDGMENTS

S.A.P., K.R.C., and A.J.C. thank the National Science Foundation−Center for Hierarchical Manufacturing (NSF−CHM CMMI-1025020) at the University of Massachusetts−Amherst for funding. M.D.B. and A.J.C. acknowledge the UMass CVIP Technology Development Fund and the Human Frontiers Science Program for financial support.

REFERENCES

(1) Greiner, C.; del Campo, A.; Arzt, E. Adhesion of Bioinspired Micropatterned Surfaces: Effects of Pillar Radius, Aspect Ratio, and Preload. *Langmuir* **2007**, *23*, 3495−3502.

(2) Murphy, M. P.; Aksak, B.; Sitti, M. Adhesion and Anisotropic Friction Enhancements of Angled Heterogeneous Micro-Fiber Arrays with Spherical and Spatula Tips. *J. Adhes. Sci. Technol.* **2007**, *21*, 1281−1296.

(3) Jagota, A.; Hui, C. Y.; Glassmaker, N. J.; Tang, T. Mechanics of Bioinspired and Biomimetic Fibrillar Interfaces. *MRS Bull.* **2007**, *32*, 492−495.

(4) Gorb, S. N. Biological Attachment Devices: Exploring Nature's Diversity for Biomimetics. *Philos. Trans. R. Soc., A* **2008**, *366*, 1557−1574.

(5) Shen, L.; Glassmaker, N. J.; Jagota, A.; Hui, C. Y. Strongly Enhanced Static Friction Using a Film-Terminated Fibrillar Interface. *Soft Matter* **2008**, *4*, 618−625.

(6) Drotlef, D. M.; Stepien, L.; Kappl, M.; Barnes, W. J. P.; Butt, H. J.; del Campo, A. Insights into the Adhesive Mechanisms of Tree Frogs Using Artificial Mimics. *Adv. Funct. Mater.* **2013**, *23*, 1137−1146.

(7) Crosby, A. J.; Hageman, M.; Duncan, A. Controlling Polymer Adhesion with "Pancakes". *Langmuir* **2005**, *21*, 11738−11743.

(8) Thomas, T.; Crosby, A. J. Controlling Adhesion with Surface Hole Patterns. *J. Adhes.* **2006**, *82*, 311−329.

(9) Chan, E. P.; Ahn, D.; Crosby, A. J. Adhesion of Patterned Reactive Interfaces. *J. Adhes.* **2007**, *83*, 473−489.

(10) Kundu, S.; Davis, C. S.; Long, T.; Sharma, R.; Crosby, A. J. Adhesion of Nonplanar Wrinkled Surfaces. *J. Polym. Sci., Part B: Polym. Phys.* **2010**, *49*, 179−185.

(11) Chan, E. P.; Smith, E. J.; Hayward, R. C.; Crosby, A. J. Surface Wrinkles for Smart Adhesion. *Adv. Mater.* **2008**, *20*, 711−716.

(12) Kwak, M. K.; Pang, C.; Jeong, H. E.; Kim, H. N.; Yoon, H.; Jung, H. S.; Suh, K. Y. Towards the Next Level of Bioinspired Dry Adhesives: New Designs and Applications. *Adv. Funct. Mater.* **2011**, *21*, 3606−3616.

(13) Pang, C.; Kang, D.; Kim, T. I.; Suh, K. Y. Analysis of Preload-Dependent Reversible Mechanical Interlocking Using Beetle-Inspired Wing Locking Device. *Langmuir* **2012**, *28*, 2181−2186.

(14) Shahsavan, H.; Zhao, B. X. Conformal Adhesion Enhancement on Biomimetic Microstructured Surfaces. *Langmuir* **2011**, *27*, 7732−7742.

(15) Vajpayee, S.; Khare, K.; Yang, S.; Hui, C. Y.; Jagota, A. Adhesion Selectivity Using Rippled Surfaces. *Adv. Funct. Mater.* **2011**, *21*, 547−555.

(16) Chung, J. Y.; Chaudhury, M. K. Roles of Discontinuities in Bio-Inspired Adhesive Pads. *J. R. Soc., Interface* **2005**, *2*, 55−61.

(17) Murphy, M. P.; Kim, S.; Sitti, M. Enhanced Adhesion by Gecko-Inspired Hierarchical Fibrillar Adhesives. *ACS Appl. Mater. Interfaces* **2009**, *1*, 849−855.

(18) Lee, J.; Bush, B.; Maboudian, R.; Fearing, R. S. Gecko-Inspired Combined Lamellar and Nanofibrillar Array for Adhesion on Nonplanar Surface. *Langmuir* **2009**, *25*, 12449−12453.
(19) Verneuil, E.; Ladoux, B.; Buguin, A.; Silberzan, P. Adhesion on Microstructured Surfaces. *J. Adhes.* **2007**, *83*, 449−472.
(20) Degrandi-Contraires, E.; Poulard, C.; Restagno, F.; Leger, L. Sliding Friction at Soft Micropatterned Elastomer Interfaces. *Faraday Discuss.* **2012**, *156*, 255−265.
(21) Yu, J.; Chary, S.; Das, S.; Tamelier, J.; Pesika, N. S.; Turner, K. L.; Israelachvili, J. N. Gecko-Inspired Dry Adhesive for Robotic Applications. *Adv. Funct. Mater.* **2011**, *21*, 3010−3018.
(22) Bartlett, M. D.; Croll, A. B.; King, D. R.; Paret, B. M.; Irschick, D. J.; Crosby, A. J. Looking Beyond Fibrillar Features to Scale Gecko-Like Adhesion. *Adv. Mater.* **2012**, *24*, 1078−1083.
(23) Bartlett, M. D.; Croll, A. B.; Crosby, A. J. Designing Bio-Inspired Adhesives for Shear Loading: From Simple Structures to Complex Patterns. *Adv. Funct. Mater.* **2012**, *22*, 4985−4992.
(24) Pendergraph, S. A.; Bartlett, M. D.; Carter, K. R.; Crosby, A. J. Opportunities with Fabric Composites as Unique Flexible Substrates. *ACS Appl. Mater. Interfaces* **2012**, *4*, 6640−6645.
(25) Paretkar, D. R.; Bartlett, M. D.; McMeeking, R.; Crosby, A. J.; Arzt, E. Buckling of an Adhesive Polymeric Micropillar. *J. Adhes.* **2013**, *89*, 140−158.
(26) Shull, K. R. Contact Mechanics and the Adhesion of Soft Solids. *Mater. Sci. Eng., R* **2002**, *36*, 1−45.